UDK 539.42
Original scientific article/Izvirni znanstveni članek

ISSN 1580-2949
MTAEC9, 47(4)441(2013)

BEHAVIOUR OF SHORT CRACKS EMANATING FROM TINY DRILLED HOLES

VEDENJE KRATKIH RAZPOK, KI NASTANEJO IZ MAJHNIH IZVRTIN

Vladimir Gliha[1], Pavlo Maruschak[2], Tomaž Vuherer[1]

[1]University of Maribor, Faculty of Mechanical Engineering, Smetanova 17, 2000 Maribor, Slovenia
[2]Ternopil Ivan Pul'uj National Technical University, Ruska 56, 46001 Ternopil, Ukraine
vladimir.gliha@um.si

Prejem rokopisa – received: 2012-10-15; sprejem za objavo – accepted for publication: 2012-11-27

Specimens with martensitic microstructure were defected by tiny drilled holes with the existing local residual stresses induced by drilling and without them. The objective of this research was to determine the cyclic stress level for the crack initiation and fatigue limit of the defected and smooth specimens' dependence upon the residual-stress field. Compressive residual stresses retarded the crack initiation. Immediately after the crack initiation, residual stresses decelerated the short-crack propagation, but later, when the residual-stress sign was changed, they accelerated it. Non-propagating short-crack size and fatigue limit also depend on the residual-stress field.

Keywords: small defect, drilled hole, crack initiation, crack propagation, short crack, long crack, anomalous fast-crack propagation

Pri preizkušancih z martenzitno mikrostrukturo smo naredili majhne izvrtine z obstoječimi lokalnimi zaostalimi napetostmi zaradi vrtanja in brez njih. Namen te raziskave je bilo določiti odvisnost ciklične napetosti, ki je potrebna za nastanek razpoke, in odvisnost trajne dinamične trdnosti z izvrtino oslabljenih in gladkih preizkušancev, od polja zaostalih napetosti. Tlačne zaostale napetosti so zavrle nastanek razpoke. Takoj po nastanku razpoke so zaostale napetosti upočasnile širjenje kratke razpoke, pozneje, ko se je predznak napetosti spremenil, pa so ga pospešile. Velikost kratke razpoke, ki se ne širi več, in trajna dinamična trdnost sta prav tako odvisni od polja zaostalih napetosti.

Ključne besede: majhne napake, izvrtina, nastanek razpoke, širjenje razpoke, kratka razpoka, dolga razpoka, nenormalno hitro širjenje razpoke

1 INTRODUCTION

The phenomenon of crack initiation from small defects in metals caused by cyclic stress at a level lower than the fatigue limit, in connection with the initial fatigue-crack propagation to the size when it becomes a non-propagating crack is now well understood.[1–3] The hardness and the defect size are crucial for the fatigue limit of the metals with small defects.[4,5] The measure of the defect size is the square root of its projection onto the plane of cyclic stress, i.e., the parameter $\sqrt{\text{area}}$. The measure of hardness is the HV number.

However, most of the experiments confirming the above-mentioned relation have been performed on specimens with small, three-dimensional, artificial surface defects. The effects of the eventual residual stresses due to the artificial defect preparation have not been taken into account. Of course, the local residual stresses induced by drilling, scratching, impressing, etc., affect the crack initiation and the initial fatigue-crack propagation. The latter is known as the short-crack propagation. Acceleration or retardation of a crack initiation and assistance or obstruction of the short-crack propagation are reflected in the sizes of the largest non-propagating cracks emanating from small defects.[5,6]

The influence of the local residual stresses caused by Vickers-pyramid indenting in an artificially prepared martensitic microstructure on the crack initiation and subsequent propagation was the matter of our previous paper.[7] We have found that these stresses play an important role in the crack initiation from Vickers indentations and its initial propagation. Actually, at the very beginning, the tensile residual stresses around both exposed corners of an indentation accelerate the initiation of two cracks along the edges. Later on, the compressive residual stresses around the top of the indentation retard the short-crack propagation along the edges in the direction towards the top. When both cracks are linked and become a single crack, which is larger than individual short cracks, it starts to behave as a long crack. Now, the tensile residual stresses around the corners accelerate the crack propagation at the surface. This large crack also assists the crack penetration into the depth. As a result, the indentations with present local residual stresses seem to be smaller than expected.[4,7]

The experimental results of the crack initiation from tiny drilled holes, instead of Vickers indentations, as well as the fatigue limits of smooth and defected specimens with identical microstructures are shown in the present article. The stress level for the crack initiation was experimentally assessed. On the specimens in the as-drilled condition, crack sizes at different stress levels were measured in order to analyse the effects of the residual-stress field on the short-crack-propagation rate.

2 EXPERIMENTAL WORK

2.1 Samples and specimen preparation

Samples of the material with martensite microstructure were used for experimental work. The chemical composition and the mechanical properties of this material are given in **Tables 1** and **2**.

Table 1: Chemical composition of the material (mass fractions, *w*/%)
Tabela 1: Kemijska sestava materiala (masni deleži, *w*/%)

C	Si	Mn	P	S	Cr	Ni	Cu	Mo	Al
0.18	0.22	0.43	0.012	0.028	1.56	1.48	0.15	0.28	0.023

Table 2: Mechanical properties of the material
Tabela 2: Mehanske lastnosti materiala

R_{p02}/ MPa	R_m/ MPa	A_5/ %	Z/ %	Impact toughness (at +20 °C)/J	Hardness/ (HV10)
1042	1431	15	56	72	463

A two-step heat treatment was used to create the microstructure of the samples. It is schematically shown in **Figure 1** (the solid line). The first stage of the heat treatment is long-lasting high-temperature annealing and water quenching (mark b), while the second stage is hardening by water quenching (d). The grains have grown during the annealing. The martensite transformation was a result of water quenching (**Figure 2**).

Cylinders were machined from the as-delivered steel 17CrNiMo7 (mark a). In the first sequence of the specimen preparation high-temperature annealing and quenching were applied (b), and then the cylinders were turned to produce grooved cylinders (c). The grooved area was fine polished.

The first sequence of the specimen preparation was the same for all the specimens. In the second sequence of

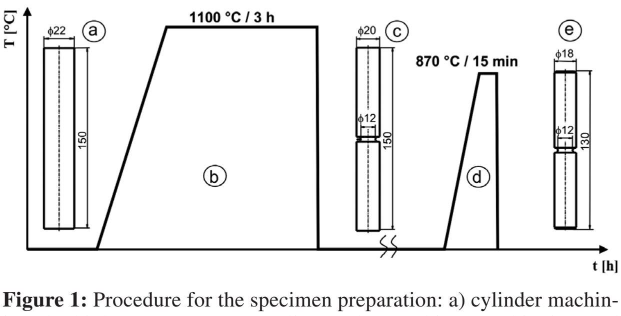

Figure 1: Procedure for the specimen preparation: a) cylinder machining, b) high-temperature annealing and quenching, c) thinning and machining a groove with ρ = 2 mm, d) hardening, e) specimen aligning by thinning and shortening
Slika 1: Postopek priprave preizkušancev: a) izdelava valja, b) visokotemperaturno žarjenje in kaljenje, c) tanjšanje in izdelava žleba z ρ = 2 mm, d) kaljenje, e) poravnavanje preizkušancev s tanjšanjem in krajšanjem

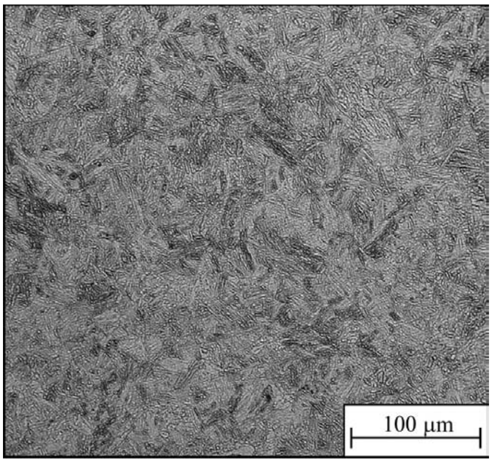

Figure 2: Microstructure of the material samples
Slika 2: Mikrostruktura vzorcev materiala

the specimen preparation, three different types of grooved cylinders were produced, i.e., type-I, type-II and type-III specimens.

I. The grooved cylinders were hardened (d), while the surface at the bottom of the groove remained intact. The type I-specimens were smooth and in the residual-stress-free condition.
II. Before hardening the cylinders were hole-drilled at the bottom of the groove. The diameter of the hole was 90 µm, while the depth was 45 µm. The local residual stresses induced by hole-drilling were relaxed due to heating over the A_{c3} temperature during the hardening (d). The type-II specimens were defected in the residual-stress-free condition.
III. The hardening (d) was followed by groove polishing and hole drilling. Therefore, the local residual-stress field induced by drilling existed in the specimens. The type-III specimens were defected and were in the as-drilled condition.

The cylinders were slightly distorted after the second sequence of the specimen preparation. In order to avoid any possible influence on the stress level during the loading, the cylinders were turned, in the third sequence of the specimen preparation, to the final size and shape (mark e). The axis of the specimens was adjusted to the centre of the existing groove. The final stress-concentration coefficient was 1.73.[8] At the end of the specimen preparation the grooves were cleaned to make the surface suitable for observations.

The specimens were loaded, at room temperature, onto the rotary bending machine with a ratio $R = -1$. The levels, at which the crack initiated from the tiny drilled hole and began to propagate, were determined experimentally. The bottom of the groove was analysed after every stop using a light microscope mounted on the loading machine. SEM was used on the dismounted specimens. The fatigue limit was defined as 10^7 cycles strength.

2.2 Cracks registration

The type-I specimens were smooth at the bottom of the groove, i.e., without small defects:

A photograph of small cracks in the type-I specimen at the stress level lower than the fatigue limit is shown in **Figure 3a**. The cracks are non-propagating. Their size is $2a$ = 50–60 μm.

A photograph of larger non-propagating cracks at the stress level higher than the former one and equal to the fatigue limit is shown in **Figure 3b**. A net of small individual cracks can be seen. The size of the largest one is $2a \cong 300$ μm. All the other ones are minor cracks.

The type-II specimens were defected by tiny holes. They were in the residual-stress-relaxed condition:

A photograph of the specimen with the drilled hole at the bottom of the groove at the stress level lower than the level for the crack initiation is shown in **Figure 4a**. There is no crack initiated.

A photograph of the specimen at the stress level above the level for the crack initiation is shown in **Figure 4b**. The cracks on both sides of the hole are non-propagating. The cracks including the hole behave as a single short, non-propagating crack. Its size is $2a$ = 165 μm.

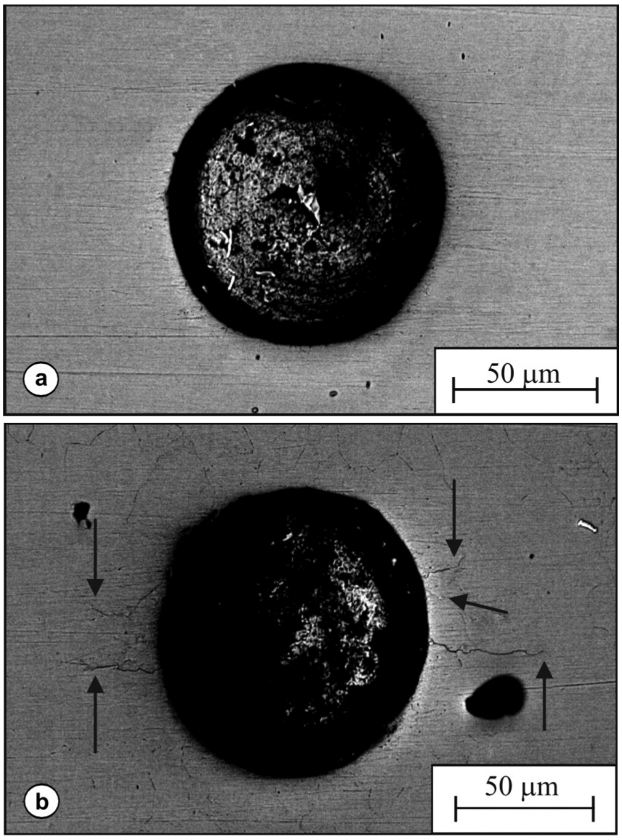

Figure 4: Two different stages at the bottom of the groove in the type-II specimens after 10^7 cycles: a) no cracks at the stress level of 357 MPa, b) non-propagating cracks at the stress level of 405 MPa

Slika 4: Dve različni stanji na dnu žleba pri preizkušancih tipa II: a) brez razpok na nivoju napetosti 357 MPa, b) razpoke, ki se ne širijo na nivoju napetosti 405 MPa

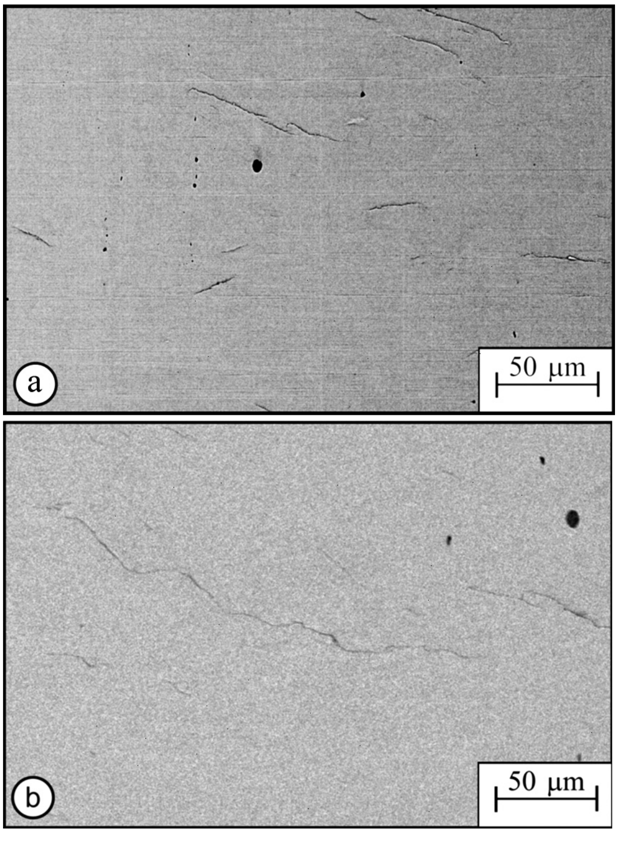

Figure 3: Non-propagating short cracks in the type-I specimens after 10^7 cycles: a) individual cracks at the stress level of 708 MPa, b) a net of cracks at the stress level of 760 MPa

Slika 3: Kratke razpoke, ki se ne širijo, pri preizkušancih tipa I po 10^7 ciklih: a) posamezne razpoke na nivoju napetosti 708 MPa, b) mreža razpok na nivoju napetosti 760 MPa

The type-III specimens were in the as-drilled condition, i.e., with the existing residual stresses:

A photograph of the initiated crack is shown in **Figure 5a**. Only one extremely short crack is registered. The crack including the hole behaves as a single short, non-propagating crack. Its length is $2a$ = 109.5 μm.

A photograph of the cracks at the stress level slightly higher than the fatigue limit is shown in **Figure 5b**. Two cracks were initiated at each side of the hole. The cracks including the hole behave as a single, but propagating crack. In this moment its size is $2a$ = 202 μm. Afterwards, the loading was continued. The specimen finally fractured before 10^7 cycles.

2.3 Short-crack analysis

In order to register the short-crack propagation in the specimens with the existing residual-stress field induced by hole-drilling and evaluate short-crack-propagation rate, some of the specimens were tested in detail at the stress levels between the levels for the crack initiation and the fatigue limit. One of the specimens was tested a

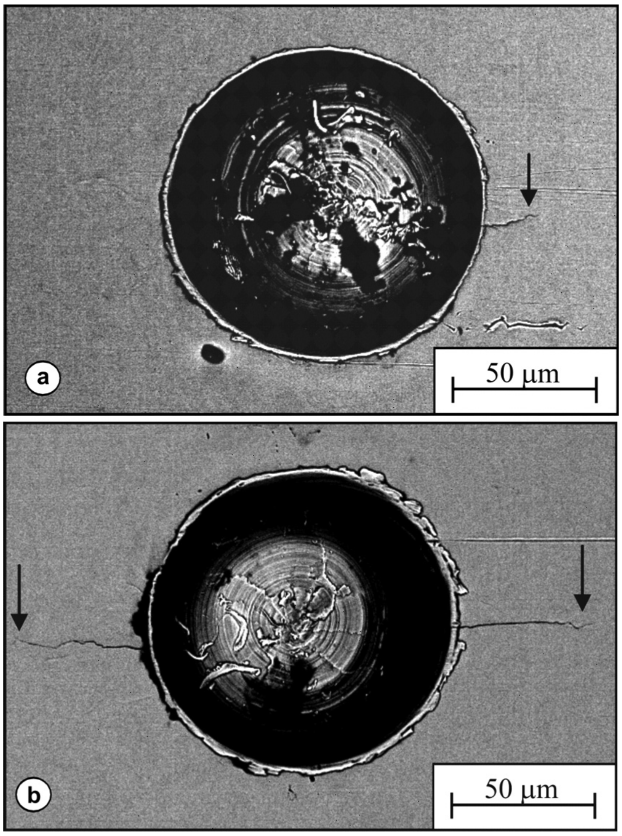

Figure 5: Two different stress levels applied to the type-III specimens: a) non-propagating crack at the stress level of 565 MPa after 10^7 cycles, b) propagating cracks at the stress level of 685 MPa after 1.27 10^6 cycles

Slika 5: Dva različna nivoja napetosti pri preizkušancih tipa III: a) razpoka, ki se ne širi, na nivoju napetosti 565 MPa po 10^7 ciklih, b) razpoki, ki se širita, na nivoju napetosti 685 MPa po 1,27 $\cdot 10^6$ ciklih

bit above the fatigue limit. The crack lengths at different stress levels and at different numbers of stress cycles were measured using microscopes.

The registered crack lengths, i.e., the sum of the single crack and the hole diameter or the sum of two cracks and the hole diameter are presented in **Figure 6** depending on the specific number of the cycles.

3 RESULTS AND DISCUSSION

3.1 Fatigue limit

The summarized data on the fatigue limit, the stress level for the crack initiation and the non-propagating crack size registered during the testing as well as the parameter $\sqrt{\text{area}}$ of the drilled holes and the information about the local residual-stress field are listed in **Table 3**. The surface stress at the bottom of the groove corresponds to the nominal bending stress multiplied by the stress-concentration coefficient.

The fatigue limit of defected specimens is lower than the fatigue limit of smooth specimens. Tiny holes help crack initiation. Cracks appear at lower stress levels. The reason for it is the stress concentration caused by a hole.

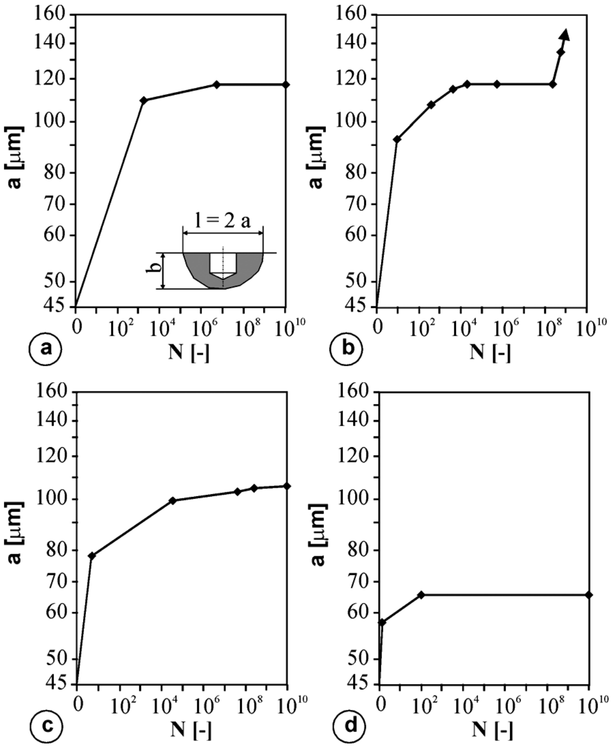

Figure 6: Dependences of crack lengths, *a*, upon the number of stress cycles, *N*, at different stress levels, *σ*: a) 697 MPa, b) 678 MPa, c) 677 MPa, d) 522 MPa

Slika 6: Odvisnost dolžin razpoke *a* od števila ciklov napetosti *N* na različnih nivojih napetosti *σ*: a) 697 MPa, b) 678 MPa, c) 677 MPa, d) 522 MPa

Table 3: Test results

Tabela 3: Rezultati preizkušanja

Specimen	Fatigue limit (MPa)	Stress level for initiation (MPa)	Non-propagating crack size (μm)	Parameter $\sqrt{\text{area}}$ (μm)	Residual stress
Type I	760	691	>150	0	none
Type II	706	381	136	56.2	none
Type III	678	517	112	58.0	present

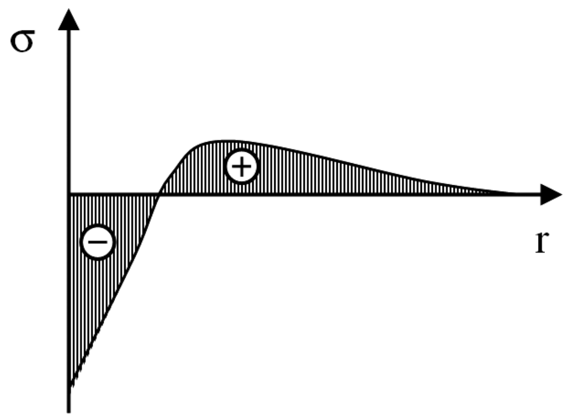

Figure 7: Course of the circular stress induced by drilling *σ*, against the distance, *r* (schematically)

Slika 7: Potek krožne napetosti *σ*, ki je nastala z vrtanjem, glede na razdaljo *r* (shematsko)

In respect to the residual-stress field induced by drilling the defected specimens behave differently. Namely, the residual stresses are compressive adjacent to the hole. Residual stresses are self-balancing forces. Compressive stresses are in the equilibrium with tensile ones. Therefore, the compressive residual stress decreases with the distance and turns to the tensile stress. The tensile stress attains its maximum at a certain distance and then it decreases. The sketch of the residual stresses induced by hole-drilling is shown in **Figure 7**.

The stress level for the crack initiation is the lowest for the type-III specimens. The largest non-propagating crack is the shortest in the type-III specimens, too. The reason can only be the existing residual-stress field. Compressive stresses retard the crack initiation.

3.2 Anomalous fast short-crack propagation

After the initiation, the short-crack propagation is anomalous fast, much faster than the propagation of the long cracks close to the threshold.

Between two successive moments during the cyclic loading of the specimens when the crack-length measurement was performed (**Figure 6**), the average crack-propagation rate was calculated as:

$$\frac{\mathrm{d}a}{\mathrm{d}N}=\frac{a_i-a_{i-1}}{N_i-N_{i-1}} \qquad (1)$$

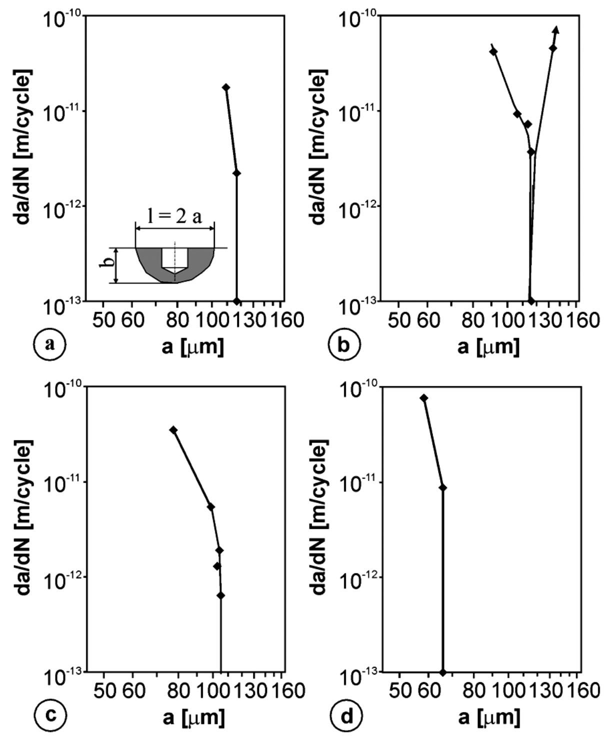

Figure 8: Dependences of the crack-propagation rate, d*a*/d*N*, upon the crack size, *a*, for different stress levels, *σ*: a) *σ* = 697 MPa, b) *σ* = 678 MPa, c) *σ* = 677 MPa, d) *σ* = 522 MPa

Slika 8: Odvisnost hitrosti širjenja razpoke d*a*/d*N* od velikosti razpoke *a* pri različnih nivojih napetosti *σ*: a) 697 MPa, b) 678 MPa, c) 677 MPa, d) 522 MPa

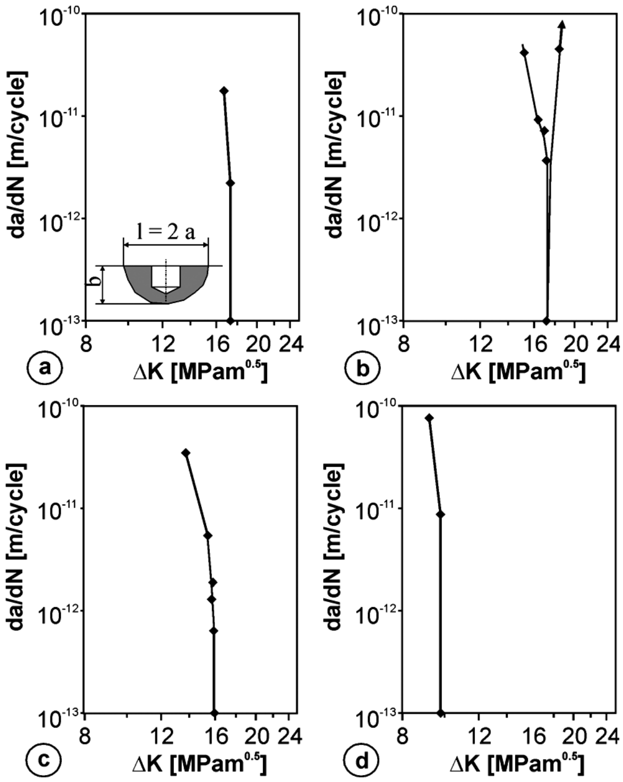

Figure 9: Dependences of the crack-propagation rate, d*a*/d*N*, upon the stress-intensity-factor range, Δ*K*, for different stress levels, *σ*: a) 697 MPa, b) 678 MPa, c) 677 MPa, d) 522 MPa

Slika 9: Odvisnost hitrosti širjenja razpoke d*a*/d*N* od razpona faktorja intenzitete napetosti Δ*K* pri različnih nivojih napetosti *σ*: a) 697 MPa, b) 678 MPa, c) 677 MPa, d) 522 MPa

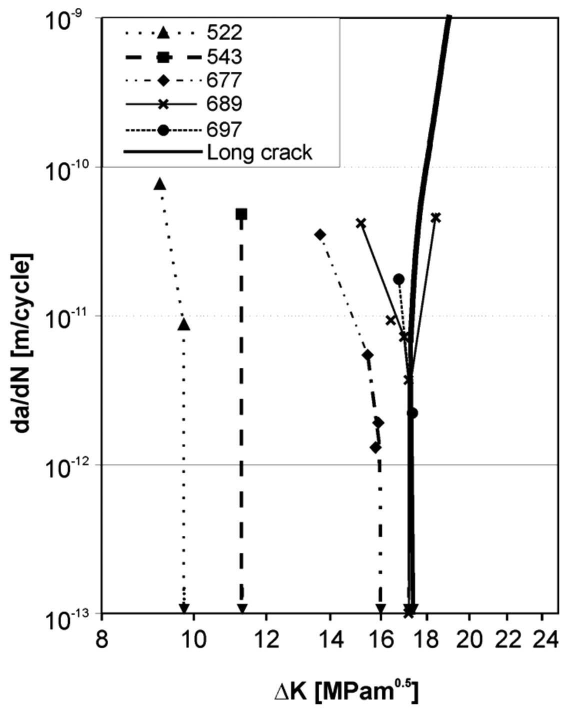

Figure 10: Comparison of short-crack and long-crack propagation rates

Slika 10: Primerjava hitrosti širjenja kratkih in dolgih razpok

The results of the calculations shown against the crack size are presented in **Figure 8**.

As expected, the short-crack-propagation rate decreases with the crack length. At the stress levels lower than the fatigue limit, the cracks sooner or later stop propagating. The crack at the stress level equal to the fatigue limit is the largest non-propagating crack.

However, the driving force for the crack propagation is the stress-intensity-factor range, ΔK:[4,6]

$$\Delta K = 0.65 \cdot \Delta\sigma \cdot \sqrt{\pi \cdot a} \quad (2)$$

The crack-propagation rates against the stress-intensity-factor range are plotted in **Figure 9**.

The comparison of all the short-crack-propagation rates with the long-crack-propagation rate[7,8] close to the threshold value for the long-crack propagation and above it are shown in **Figure 10**. The largest non-propagating crack in the type-III specimens is 112 μm long (the sum of the cracks and the hole diameter is 224 μm).

The reason why the non-propagating cracks in the type-III specimens are not as large as the ones in the type-II specimens is the stress field induced by hole-drilling. At the stress levels much lower than the fatigue limit, a short crack begins to propagate through the domain of compressive residual stresses. These levels lower ΔK_{eff} as well as the short-crack propagation rate. Due to the decreasing compressive residual stress during the crack propagation, the crack closure decreases and ΔK_{eff} increases. The result is the quickly increasing short-crack propagation. Despite the decelerated initial crack propagation due to the compressive residual-stress field, the crack, sooner or later, propagates to the domain of the tensile residual stress. Then the crack propagates faster. The largest non-propagating crack in the type-III specimens is therefore smaller than in the type-II specimens.

4 CONCLUSIONS

Immediately after the initiation the driving force for the short-crack propagation is not equal to the whole stress-intensity-factor range, ΔK, but to its effective range, ΔK_{eff}. The reason is the crack-closure effect. As a short crack approaches the grain boundary, the propagation rate is gradually retarded because ΔK_{eff} decreases. If the stress level of the applied cyclic stress is lower than the fatigue limit, i.e., ΔK_{eff} is smaller than the threshold stress-intensity-factor range, the crack stops propagating and becomes a non-propagating crack.[9] In contrast, if ΔK_{eff} is bigger than the threshold value, the crack will continue to propagate as a long crack after retardation during the short-crack propagation.

The largest non-propagating crack in the type-I specimens is longer than in the type-II specimens. Both specimen types are in the residual-stress-free condition. A drilled hole makes a crack initiation easy. The registered crack in a type-I specimen is the largest crack spreading along the whole circumference of the specimen, while the crack in a type-II specimen was forced to emanate from the drilled hole. It is expected that the condition for the unimpeded short-crack propagation is not so convenient in the type-II specimens because short-crack propagation depends on the grain composition (size, orientation etc).

5 REFERENCES

[1] K. J. Miller, The behavior of short fatigue cracks and their initiation 1. A review of 2 recent books, Fatigue & Fracture of Engineering Materials & Structures, 10 (**1987**) 1, 75–91

[2] K. J. Miller, The behavior of short fatigue cracks and their initiation 2. A general summary, Fatigue & Fracture of Engineering Materials & Structures, 10 (**1987**) 2, 93–113

[3] Y. Murakami, M. Endo, Effects of defects, inclusions and inhomogeneities on fatigue-strength, International Journal of Fatigue, 16 (**1994**) 3, 163–182

[4] Y. Murakami, M. Endo, Quantitative evaluation of fatigue strength of metals containing various small defects or cracks, Engineering Fracture Mechanics, 17 (**1983**), 1–15

[5] Y. Murakami, M. Endo, Effect of hardness and Crack geometries on ΔK_{th} of small cracks estimating from small defect, In K. J. Miller, E. R. de los Rios, editors, Proceedings, The behaviour of short fatigue cracks, Mechanical Engineering Publications, London 1986, 275–294

[6] Y. Murakami, K. J. Miller, What is fatigue damage? A view point from the observation of low cycle fatigue process, International Journal of Fatigue, 27 (**2005**) 3, 991–1005

[7] T. Vuherer, L. Milović, V. Gliha, Behaviour of small cracks during their propagation from Vickers indentations in coarse-grain steel: An experimental investigation, International Journal of Fatigue, 33 (**2011**) 12, 1505–1513

[8] T. Vuherer, Analysis of influence of micro defects on fatigue strength of coarse grain HAZ in welds, Doctor Thesis, University of Maribor, Faculty of Mechanical Engineering, 2008

[9] S. Suresh, Fatigue of materials, second edition, Cambridge University Press, Cambridge 1998, 343–345, 541–569